SCIENCE CHINA
Information Sciences

• RESEARCH PAPER •

March 2024, Vol. 67, Iss. 3, 132206:1–132206:12
https://doi.org/10.1007/s11432-023-3848-6

Optimizing evasive maneuvering of planes using a flight quality driven model

Chang LIU[1], Shaoshan SUN[2], Chenggang TAO[2], Yingxin SHOU[1] & Bin XU[1*]

[1]*School of Automation, Northwestern Polytechnical University, Xi'an* 710072*, China;*
[2]*Chengdu Aircraft Design & Research Institute of AVIC, Chengdu* 610041*, China*

Received 5 March 2023/Revised 14 May 2023/Accepted 2 August 2023/Published online 26 February 2024

Abstract This paper investigates the optimal evasive maneuver for a plane to avoid an incoming missile. To accurately model the system dynamics while improving computational efficiency, a simplified plane model based on flight quality is established. A missile model with proportional guidance is also formulated. The problem of determining the optimal evasion plane maneuver is formulated. The Gauss pseudospectral method (GPM) is proposed as a solution to find the optimal maneuver. The optimized maneuver is validated by testing it on a high-fidelity 6-degree-of-freedom (6-DOF) model, which demonstrates the effectiveness of the proposed simplified plane model. The Monte Carlo method is employed to evaluate the capability of the plane to evade missiles in various scenarios and elucidate general principles for successful evasion.

Keywords optimal maneuver, flying quality, evasive strategy, pursuit-evasion game, air-to-air combat

1 Introduction

Intelligent air combat has the potential to significantly reduce the operational burden on pilots, allowing them to focus more on critical decision-making tasks. As such, research on air combat extends beyond-visual-range air combat [1–5], within-visual-range air combat [6–9], and multi-agent air combat [1, 10–13], among others. In particular, the plane-versus-missile (PVM) problem is a prominent topic in air combat research. In PVM scenarios, the primary objective of the plane is to evade the incoming missile, while the missile's goal is to intercept the plane. Due to the high relative velocity and short distance between the two, the plane must perform significant maneuvers to avoid a collision with the missile. Maneuver selection based on the library and maneuver generation based on computation are two research approaches to solving the PVM problem.

For maneuver selection based on library, a pre-established library is used to generate the evasive maneuver of the plane [14–17]. NASA proposes that the most common flying maneuvers comprise seven elemental movements, including max load left turn, max load right turn, max acceleration, steady flight, max deceleration, max load pull up, and max load push over [18]. It is assumed that more complex maneuvers are constructed from elemental movements, and the plane must select the appropriate maneuver from its library based on the current circumstances. In [19], the optimal sequence of elemental maneuvers is generated using a hierarchical decision-making structure. However, the selection of elemental movements is dependent on situation assessment and threat estimation algorithms, which require expert knowledge. To address air combat decision-making, a maneuver decision strategy based on deep reinforcement learning is proposed in [20]. Nonetheless, completing the flight using the sequence of elemental maneuvers alone is highly risky and may not ensure the necessary maneuver flexibility for PVM scenarios.

For maneuver generation based on computation, the PVM model calculates the evasive maneuver of the plane [21–23]. In [24, 25], the optimal evasive maneuvers for a plane facing a surface-to-air missile are investigated. Differential game theory is employed in [26] to solve a set of local solutions to the PVM problem, and the concept of energy maneuverability is introduced to assist in finding the global optimal

* Corresponding author (email: smileface.binxu@gmail.com)

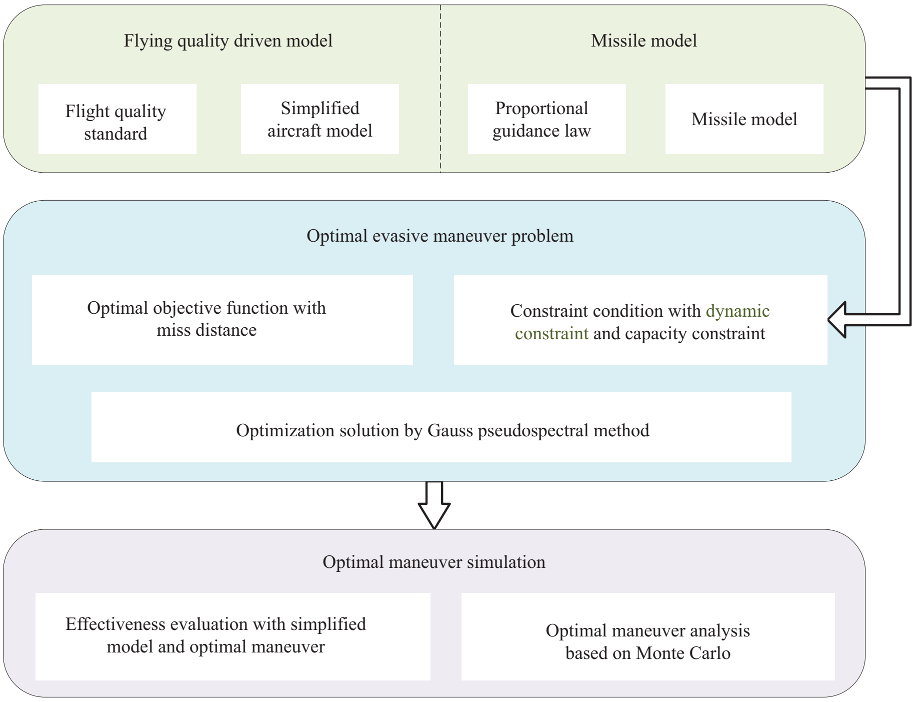

Figure 1 (Color online) System diagram of the optimal evasive maneuver.

solution. In [27], the proportional navigation is considered nearly optimal for the pursuer, and the one-sided optimal control problem is established and solved using the semi-direct nonlinear programming method. In [28], a tail chase scenario between two aircraft is assumed, where the attacker attempts to shoot down the evader with two missiles, while the evader performs optimal maneuvers to avoid the missiles. In [29], optimal coordinated maneuvers for resolving conflicts among multiple aircraft are proposed, and a numerical algorithm for computing the optimal resolution maneuvers is presented.

The accurate modeling of the plane and missile dynamics is crucial for solving the optimal maneuver problem. However, the conventional particle model used to represent the dynamic constraints is limited in capturing the response characteristics and capability limits of the entire model [30]. Specifically, while the aerodynamic forces acting on the plane are considered in the model [22], the plane's normal acceleration is used as the model input, which only partially reflects the plane's performance. This simplified dynamics cannot fully capture the dynamic behavior of the model, especially during the super maneuver stage. Therefore, it is essential to employ accurate plane and missile models to recast the PVM problem as an optimal maneuver problem, which can be effectively solved using optimization algorithms [31–35].

Motivated by the need for PVM, this paper proposes a new approach by accurately modeling the plane and missile dynamics, and formulating the optimal evasion maneuver problem. The key contributions are the following:

(1) Based on the flight quality standard of a plane, a transfer function from stick force to attitude angle is proposed in this paper. And the flight quality driven model is established to directly reflect the dynamic performance of attitude response and avoid the influence of controller design.

(2) The proposed flight quality driven model is combined with missile constraints to ensure that the optimized maneuvering of the plane meets the performance and dynamic constraints of the plane. And the optimal evasive maneuver could be applied in the real 6-degree-of-freedom (6-DOF) model directly.

This paper is organized as follows. Section 2 presents the plane model based on flying quality and the missile model with proportional guidance law. In Section 3, it covers the problem of optimal evasion of plane maneuver problem and the Gauss pseudospectral method (GPM) to optimal maneuver problem. Afterward, Section 4 demonstrates and analyzes the test of the suggested algorithm. Finally, in Section 5, the conclusion is stated. Figure 1 depicts the optimal evasive maneuver diagram.

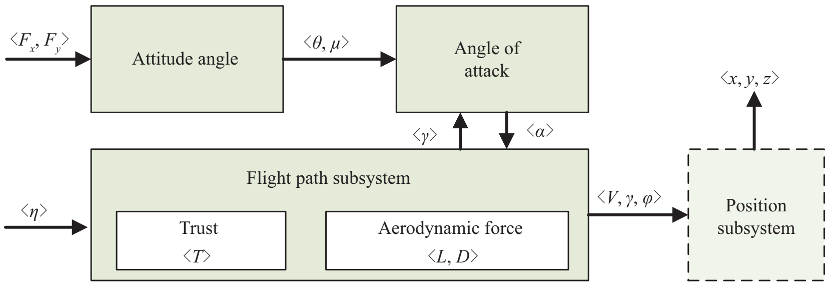

Figure 2 (Color online) Diagram of the flying quality driven model.

Table 1 Symbols and definitions in the equivalent transfer function

Symbol	Definition	Symbol	Definition
K_q	Gain of pitch rate response	K_μ	Gain of roll response
ξ_{sp}	Short-period damping ratio	ξ_μ	Damping ratio of roll response
ω_{sp}	Short-period natural frequency	ξ_d	Damping ratio of dutch roll
Z_α^*	Reciprocal of molecular time constant for pitch rate	ω_d	Natural frequency of dutch roll
τ_q	Delay constant of pitch rate response	ω_μ	Natural frequency of roll response
T_s	Time constant of spiral mode	τ_μ	Delay constant of roll response
T_R	Time constant of roll mode		

2 Mathematical model

2.1 Flying quality driven model

In this subsection, an attitude angle model is developed based on flight quality. Furthermore, the track angle and speed model are calculated using the force of the plane. The geometrical structure of the plane coordinate system is used to establish an angle of attack (AOA) model. Finally, a simplified dynamic model based on flight quality is established through the combination of the aforementioned equations. The diagram of the flying quality driven model is shown in Figure 2.

(1) Attitude angle subsystem based on flying quality. The flying quality defines the requirements for the flying and handling qualities, which are commonly utilized by plane controller engineers as guidance. Therefore, the general manned plane's flight quality was always excellent after attaching the satisfactory stability augmentation system. The model from manipulator to plane attitude is established and displayed as follows:

$$\frac{q(s)}{F_y(s)} = \frac{K_q(s+Z_\alpha^*)}{s^2+2\xi_{sp}\omega_{sp}s+\omega_{sp}^2}\mathrm{e}^{-\tau_q s}, \tag{1}$$

$$\frac{\mu(s)}{F_x(s)} = \frac{K_\mu(s^2+2\xi_\mu\omega_\mu+\omega_\mu^2)}{(s^2+2\xi_d\omega_d s+\omega_d^2)(s+\frac{1}{T_R})(s+\frac{1}{T_s})}\mathrm{e}^{-\tau_\mu s}, \tag{2}$$

where q and μ refer to the pitch rate and roll angle of the plane in the body coordinates, F_y and F_x are the stem force of pitch and roll which are considered the input of the plane.

The definitions of parameters in the equivalent transfer function (1) and (2) are shown in Table 1. The parameter of flying quality is declared in the standard MIL-1797A.

To calculate q and μ, the transform function mentioned in (1) and (2) can be converted into the form of the state equation provided as

$$\begin{aligned} \dot{x}_q &= A_q x_q + B_q u_q, \\ \dot{q} &= C_q \dot{x}_q, \end{aligned} \tag{3}$$

$$\begin{aligned} \dot{x}_\mu &= A_\mu x_\mu + B_\mu u_\mu, \\ \dot{\mu} &= C_\mu \dot{x}_\mu, \end{aligned} \tag{4}$$

where x_q and x_μ are the state variables of q and μ, respectively. $\langle A_q, B_q, C_q\rangle$ and $\langle A_\mu, B_\mu, C_\mu\rangle$ are the state matrices that are determined by the transform function (1) and (2), respectively.

The pitch angle θ can be obtained as

$$\dot{\theta} = q\cos\mu - \dot{\varphi}\sin\mu, \tag{5}$$

where $\dot{\varphi}$ will be given in (6).

Remark 1. The simplified flying quality driven model (FQM) enables the direct acquisition of dynamic response outcomes for the attitude system, unaffected by controller design.

(2) Flight path angle subsystem based on plane force. The force equation is applied to calculate the path angle and speed of a plane, which are given as

$$\begin{aligned} mV\cos\theta\dot{\varphi} &= L\sin\mu + T[\sin(\alpha+\phi_T)\sin\mu \\ &\quad - \cos(\alpha+\phi_T)\sin\beta\cos\mu], \\ mV\dot{\gamma} &= L\cos\mu - mg\cos\gamma + T[\sin(\alpha+\phi_T)\cos\mu \\ &\quad + \cos(\alpha+\phi_T)\sin\beta\sin\mu], \\ m\dot{V} &= T\cos(\alpha+\phi_T)\cos\beta - D - mg\sin\gamma, \end{aligned} \tag{6}$$

where γ is flight path angle, φ is heading angle, V represents the fligh velocity, α refers to the AOA of plane, ϕ_T refers to the engine mounting angle, β refers to the sideslip angle, T refers to the trust of engine, L refers to the lift of the plane, D refers to the drag of plane, and m refers to the mass of plane.

The lift and drag in (6) are supplied as

$$\begin{aligned} L &= \frac{1}{2}C_{\mathrm{L}}S\rho V^2, \\ D &= \frac{1}{2}C_{\mathrm{D}}S\rho V^2, \end{aligned} \tag{7}$$

where C_{L} and C_{D} represent the lift aerodynamic derivative and drag aerodynamic derivatives, respectively, S is the wing area, ρ is the air density at current altitude, and V is the speed of a plane.

The thrust of an engine is the function of throttle, altitude, and Mach number. It is believed that the plane's engine thrust is a linear function of the throttle, which may be represented as

$$T = \eta T_{\max}, \tag{8}$$

where $T_{\max}$ is the maximum thrust at current altitude and speed, $\eta \in [0,1]$ is the throttle of plane.

(3) Angle of attack. According to the definition of plane coordinates, the relationship between flight path angle, AOA, sideslip angle, pitch angle, and roll angle is given as

$$\sin\gamma = \cos\alpha\cos\beta\sin\theta - \cos\theta\sin\beta\sin\mu - \cos\theta\sin\alpha\cos\beta\cos\mu. \tag{9}$$

The AOA could obtain by solving (9), which is provided as

$$\sin\alpha = \frac{\varepsilon\sin\theta\sqrt{\cos^2\theta\cos^2\mu - \sin^2\gamma + \sin^2\theta}}{\sin^2\theta + \cos^2\theta\cos^2\mu} - \frac{\sin\gamma\cos\theta\cos\mu}{\sin^2\theta + \cos^2\theta\cos^2\mu}, \tag{10}$$

where $\varepsilon = \mathrm{sign}(\sin\theta)\mathrm{sign}(\cos\mu)$ is used to select the solution.

Remark 2. The sideslip angle β is assumed to be zero in this paper. Due to the fact that when the plane incorporates a stability augmentation system, the sideslip angle is maintained at a small and near-zero value through feedback control.

(4) Flying quality driven model. From (3)–(10), the simplified dynamics model of plane is

$$\begin{cases} \dot{x} = V\cos\gamma\cos\varphi, \\ \dot{y} = V\cos\gamma\sin\varphi, \\ \dot{z} = V\sin\gamma, \\ m\dot{V} = T\cos(\alpha+\phi_T)\cos\beta - D - mg\sin\gamma, \\ mV\dot{\gamma} = L\cos\mu - mg\cos\gamma + T[\sin(\alpha+\phi_T)\cos\mu \\ \qquad + \cos(\alpha+\phi_T)\sin\beta\sin\mu], \\ mV\cos\theta\dot{\varphi} = L\sin\mu + T[\sin(\alpha+\phi_T)\sin\mu \\ \qquad - \cos(\alpha+\phi_T)\sin\beta\cos\mu], \\ \dot{x}_\mu = A_\mu x_\mu + B_\mu u_\mu, \\ \dot{\mu} = C_\mu \dot{x}_\mu, \\ \dot{x}_q = A_q x_q + B_q u_q, \\ \dot{q} = C_q \dot{x}_q, \\ \dot{\theta} = q\cos\mu - \dot{\varphi}\sin\mu, \end{cases} \tag{11}$$

where x, y, z refer to the coordinates of the plane.

2.2 Missile model with proportional guidance law

The proportional guidance law is implemented to update the guidance heading commands U_{m_h} and U_{m_x},

$$\begin{aligned} \dot{U}_{m_h} &= U_{m_{\max}} \frac{2}{\pi} \tan^{-1}\left(\frac{\sqrt{3}n\dot{\phi}_h}{U_{m_{\max}}}\right) - U_{m_h}, \\ \dot{U}_{m_x} &= U_{m_{\max}} \frac{2}{\pi} \tan^{-1}\left(\frac{\sqrt{3}n\dot{\phi}_x}{U_{m_{\max}}}\right) - U_{m_x}, \end{aligned} \tag{12}$$

where n is the navigation constant, $U_{m_{\max}} = \frac{gG_{m_{\max}}}{V_{m_{\mathrm{const}}}}$ refers to the maximum missile guidance heading rate which is used to limit the maximum missile overload $G_{m_{\max}}$, ϕ_h and ϕ_x are the vertical and horizontal line-of-sight rotation rates calculated as

$$\begin{aligned} \dot{\phi}_h &= \frac{\frac{\Delta\dot{z}}{r_{\mathrm{hor}}} - \frac{\Delta z\Delta x\Delta\dot{x}}{r_{\mathrm{hor}}^3} - \frac{\Delta z\Delta y\Delta\dot{y}}{r_{\mathrm{hor}}^3}}{(1+\frac{\Delta z^2}{r_{\mathrm{hor}}^2})}, \\ \dot{\phi}_x &= \frac{\Delta\dot{y}\Delta x - \Delta y\Delta\dot{x}}{r_{\mathrm{hor}}^2}, \end{aligned} \tag{13}$$

where $\Delta x = x - x_m$, $\Delta y = y - y_m$, $\Delta z = z - z_m$, and $r_{\mathrm{hor}}^2 = \Delta x^2 + \Delta y^2$, x_m, y_m, and z_m refer to the coordinates of the missile.

The kinematic model of a missile is

$$\begin{cases} \dot{x}_m = V_m\cos\gamma_m\cos\varphi_m, \\ \dot{y}_m = V_m\cos\gamma_m\sin\varphi_m, \\ \dot{z}_m = V_m\sin\gamma_m, \\ \dot{\gamma}_m = U_{m_h}, \\ \dot{\varphi}_m = U_{m_x}, \\ \dot{U}_{m_h} = U_{m_{\max}} \frac{2}{\pi} \tan^{-1}\left(\frac{\sqrt{3}n\dot{\phi}_h}{U_{m_{\max}}}\right) - U_{m_h}, \\ \dot{U}_{m_x} = U_{m_{\max}} \frac{2}{\pi} \tan^{-1}\left(\frac{\sqrt{3}n\dot{\phi}_x}{U_{m_{\max}}}\right) - U_{m_x}, \end{cases} \tag{14}$$

where γ_m and φ_m are flight path angle and heading angle, respectively, V_m refers to the speed of the missile.

3 Optimal evasion maneuver based on the GPM

3.1 Optimal evasion maneuver problem

The objective of the optimal evasion plane maneuver problem is to maneuver the plane so as to avoid being struck by an oncoming missile, which can be formulated as an optimal problem. The bolza objective function of plane optimal control is

$$J(\boldsymbol{U}) = \int_{t_0}^{t_f} L(\boldsymbol{X}, \boldsymbol{U}, t)\mathrm{d}t + \varphi\left(\boldsymbol{X}_f, t_f\right), \\ \text{s.t.} \begin{cases} \dot{\boldsymbol{X}} = \boldsymbol{f}(\boldsymbol{X}, \boldsymbol{U}, t), \quad \boldsymbol{X}\left(t_0\right) = \boldsymbol{X}_0, \\ \boldsymbol{g}(\boldsymbol{X}, \boldsymbol{U}, \dot{\boldsymbol{U}}, \ddot{\boldsymbol{U}}) \leqslant \boldsymbol{0}, \end{cases} \tag{15}$$

where $\boldsymbol{X} = [x, y, z, V, \gamma, \varphi, \mu, q, \theta, x_m, y_m, z_m, \gamma_m, \varphi_m, U_{m_h}, U_{m_x}]^{\mathrm{T}}$ is the state of system containing the plane and missile states, $\boldsymbol{U} = [F_x, F_y, \eta]^{\mathrm{T}}$ is the control input of plane, $\boldsymbol{X}_0$ is the initial state, $\dot{\boldsymbol{X}} = \boldsymbol{f}(\boldsymbol{X}, \boldsymbol{U}, t)$ is the dynamic constraint of plane (11) and missile (14), $\boldsymbol{g}(\boldsymbol{X}, \boldsymbol{U}, \dot{\boldsymbol{U}}, \ddot{\boldsymbol{U}}) \leqslant \boldsymbol{0}$ is the capacity constraint which is given as

$$\alpha^L \leqslant \alpha \leqslant \alpha^M, \quad z^L \leqslant z \leqslant z^M, \quad n_a^L \leqslant n_a \leqslant n_a^M, \\ F_x^L \leqslant F_x \leqslant F_x^M, \quad F_y^L \leqslant F_y \leqslant F_y^M, \quad \eta^L \leqslant \eta \leqslant \eta^M, \tag{16}$$

where n_a is the overload, $\aleph^L$ and $\aleph^M$ represent the lower and upper bounds of the signal $\aleph$, respectively.

In this paper, the miss distance (MD) is set as the optimal objective function,

$$\max J = \max \varsigma, \quad \varsigma = \min_{0<t<t_f} \|\mathrm{dis}(t)\|, \tag{17}$$

where $\mathrm{dis}(t)$ is the function of time that determines the distance between a plane and a missile, and ς is the MD of a missile. The aim of optimal evasion maneuver problem is to identify the optimal control sequence of the plane, which could maximize the MD of a missile.

3.2 Optimal maneuver based on the optimization algorithm

The GPM [36] is utilized to solve the optimal control problem (15) in continuous time that incorporates the dynamic constraint and capacity constraint.

The state and control are discretized on the Legendre Gauss (LG) points distributing between −1 and 1. The optimal evasion problem described could be converted to the nonlinear programming problem (18), which can then be solved by the sequential quadratic programming algorithm.

$$\max J = \max \min_{0<t<t_f} \|\mathrm{dis}(t)\| \\ \text{s.t.} \begin{cases} \sum\limits_{i=0}^{N} D_{ki}(\tau)\boldsymbol{X}(\tau_i) - \frac{t_f - t_0}{2}\int_{-1}^{1} f(\boldsymbol{X}(\tau), \boldsymbol{U}(\tau), \tau)\mathrm{d}\tau = 0, \\ C(\boldsymbol{X}(\tau_i), \boldsymbol{U}(\tau_i), \tau_i; t_0, t_f) \leqslant 0, \end{cases} \tag{18}$$

where $\tau = \frac{2t}{t_f - t_0} - \frac{t_f + t_0}{t_f - t_0}$, $t \in [t_0, t_f]$, $\tau \in [-1, 1]$, t_0 is initial time, t_f is terminal time, D_{ki} is the derivative matrix of the ith Lagrange polynomial which could be determined offline as follows:

$$D_{ki} = \begin{cases} \frac{\dot{h}(\tau_k)}{(\tau_k - \tau_i)\dot{h}(\tau_i)}, & k \neq i, \\ \frac{\ddot{h}(\tau_i)}{2\dot{h}(\tau_i)}, & k = i, \end{cases} \tag{19}$$

where $\dot{h}(\tau_i) = (1 + \tau_i)(P_{N+1}(\tau_i) - P_N(\tau_i))$.

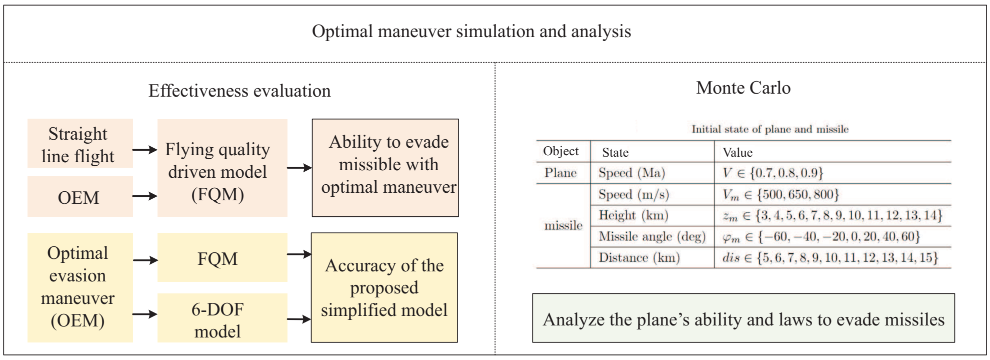

Figure 3 (Color online) Simulation and analysis of the optimal maneuver.

Table 2 Parameters of the plane

Parameter	Value	Parameter	Value
Wing area	45 m^2	Maximum trust of engine	45500 N
Mass	9100 kg	Gravitational acceleration	9.8 m/s^2
Air density	0.7787 kg/m^3		

4 Simulation

In this section, the paper carried out optimal maneuver simulation based on a simplified model, and verified the accuracy of the simplified model by comparing it with the 6-DOF model response, to ensure the effectiveness of the proposed algorithm. Furthermore, Monte Carlo methods were used to solve for the optimal maneuver under different initial states of the plane and the missile, and the ability and law of the plane's maneuver to avoid missiles were analyzed. This allowed for a thorough investigation of the ability of the proposed algorithm to effectively guide the plane safely away from incoming threats. The simulation and analysis of optimal maneuver diagram are shown in Figure 3.

4.1 Effectiveness evaluation with simplified model and optimal maneuver

The proposed simplified model and optimization algorithm are simulated in a variety of conditions. Additionally, the response of the proposed FQM under optimal evasion maneuver is defined as "FQM" whereas the response of the plane's 6-DOF model under optimal evasion maneuver is marked as "6-DOF". To verify the effectiveness of the proposed algorithm, the straight-line flight of a plane is simulated as the control group which is labeled as "SLF".

In the simulation, the proposed FQM is the simplification of ADMIRE, and the parameters are shown in Table 2. The capacity constraint of plane is considered $-15° \leqslant \alpha \leqslant 25°$, $0.3\ \text{km} \leqslant z \leqslant 15\ \text{km}$, $-1 \leqslant F_x \leqslant 1$, $-1 \leqslant F_y \leqslant 1$, $0 \leqslant \eta \leqslant 1$, and $-9 \leqslant n_a \leqslant 9$. The initial states of plane are set as $[x, y, z] = [0\ \text{km}, 0\ \text{km}, 3\ \text{km}]$, $V = 230$ m/s, and $[\theta, \mu, \varphi] = [0°, 0°, 0°]$. And the initial state of the missile are selected as $[x_m, y_m, z_m] = [10\ \text{km}, 5\ \text{km}, 13\ \text{km}]$, $V_m = 230$ m/s, and $[\theta_m, \mu_m, \varphi_m] = [0°, 0°, -135°]$.

Case 1: Simulation comparison under "FQM" and "SLF". The simulation results can be seen in Figures 4 and 5. In Figure 4, the trajectory of "FQM" is the optimal evasion maneuver calculated by the optimization algorithm, and the trajectory of "SLF" shows the positions of the plane during the straight flight maneuver. Figure 5 depicts the curve of the distance between a plane and a missile, the MD $\varsigma \geqslant 200$ under "FQM" and $\varsigma = 0$ under "SLF". The results show that the proposed FQM can evade approaching missiles by using optimal maneuvers, demonstrating the effectiveness of the proposed optimization algorithm.

Case 2: Simulation comparison under "FQM" and "6-DOF". The simulation results can be seen in Figures 6–9. The response of the 6-DOF model, which is controlled by the optimal maneuver sequence calculated by the simplified model, is displayed in Figure 6. From the side and top views in Figure 7, it can be observed that the plane performs maneuvers such as level flight, descent, left turn descent, and right turn climb at (1500 m, 0 m, 3000 m) to avoid incoming missiles. Figures 6–8 indicate that trajectories between the 6-DOF model and FQM have a high similarity, indicating that the FQM can be used as a simplified surrogate model of the 6-DOF in missile evasion scenarios.

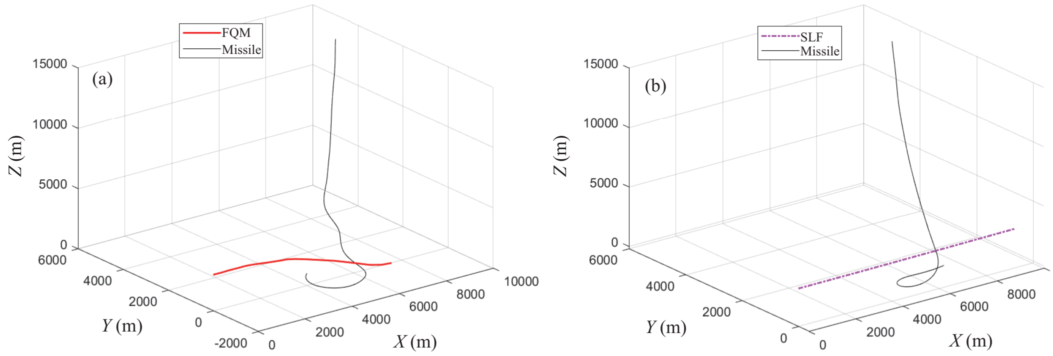

Figure 4 (Color online) 3-Dimensional trajectories of the plane and the missile. (a) Trajectories under "FQM"; (b) trajectories under "SLF".

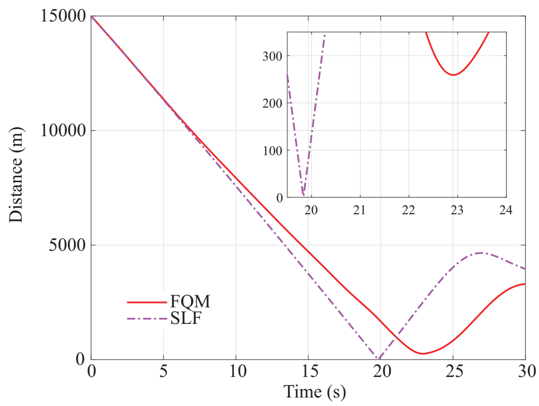

Figure 5 (Color online) Distances between the plane and the missile under "FQM" and "SLF".

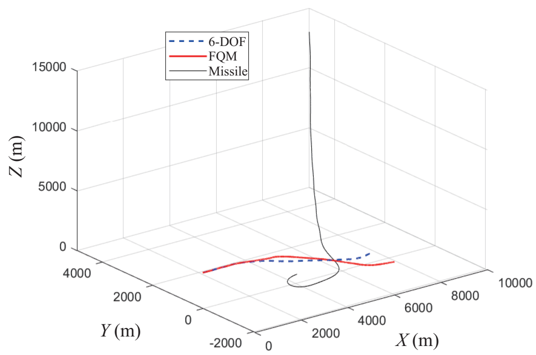

Figure 6 (Color online) 3-Dimensional trajectories under "FQM" and "6-DOF".

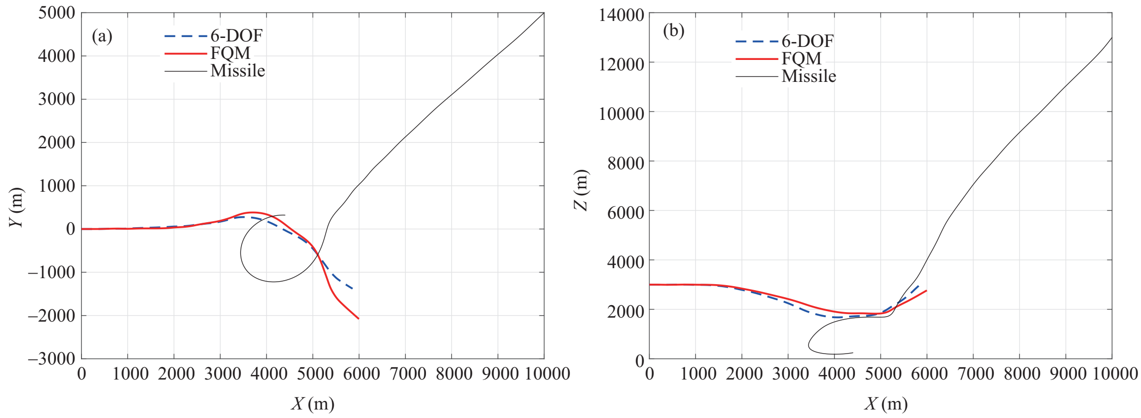

Figure 7 (Color online) Trajectories of the plane avoiding the missile under "6-DOF" and "FQM". (a) Top view; (b) side view.

The responses of the plane are presented in Figure 9. The attitude angles, velocity, and aerodynamic angles of the plane are portrayed in Figure 9. Despite the existence of inaccuracy between FQM and 6-DOF, it has been observed that the FQM response time is adequate. In a 30 s simulation, the average simulation duration of the FQM and 6-DOF is 0.093 and 7.549 s, respectively. It indicates that the running speed of the FQM is 81 times faster than that of the 6-DOF model, which suggests that the proposed FQM offers a computationally efficient inference process while still delivering comparable accuracy.

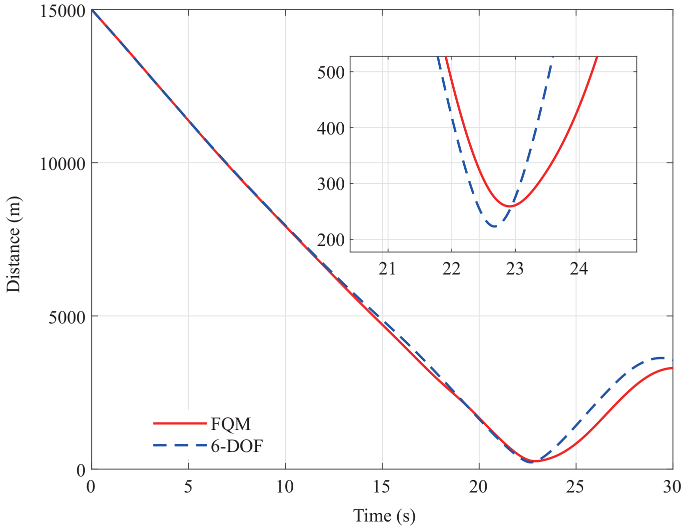

Figure 8 (Color online) Distances between the plane and the missile under "FQM" and "6-DOF".

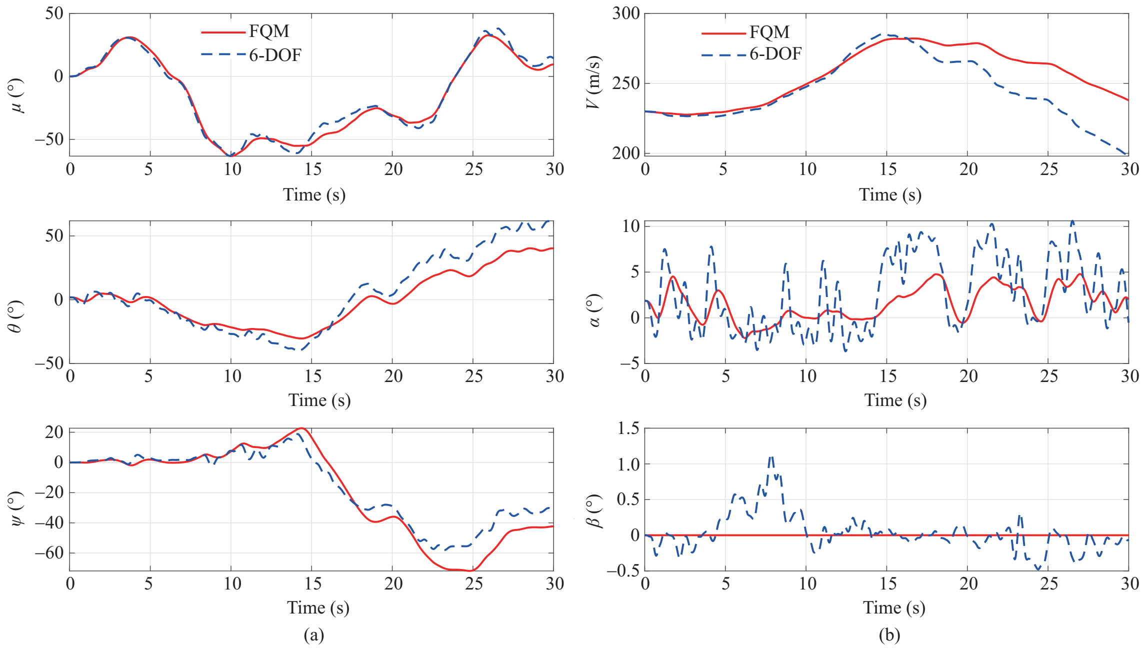

Figure 9 (Color online) Plane trajectory responses under "FQM" and "6-DOF". (a) Attitude angles; (b) velocity and aerodynamic angles.

4.2 Optimal maneuver analysis based on Monte Carlo

To analyze the evasive ability of the proposed algorithm for incoming air-defense missiles, the Monte Carlo shooting method was employed in this paper. A series of initial states of the plane and the missile were selected, the optimal maneuver solution was solved by the proposed algorithm, and the simulation results were statistically analyzed, as shown in Table 3.

The Monte Carlo simulation results of optimal maneuvering actions are shown in Figure 10. The symbols at different positions represent different initial missile positions, with the green five-pointed stars representing successful avoidance of incoming missiles, and the red triangles indicating failure of evasion.

From the scattered plots in Figures 10 and 11, it can be seen that the initial height of the missile has a considerable effect on the plane's ability to successfully maneuver to avoid it. The higher the initial height of the missile, the more time and the longer distance the plane has to respond, thus increasing its likelihood of evading the missile. Additionally, a larger approaching angle of the missile makes it harder

Table 3 Initial states of the plane and the missile

Object	State	Value
Plane	Speed (Ma)	$V \in \{0.7, 0.8, 0.9\}$
Missile	Speed (m/s)	$V_m \in \{500, 650, 800\}$
	Height (km)	$z_m \in \{3, 4, 5, 6, 7, 8, 9, 10, 11, 12, 13, 14\}$
	Missile angle (°)	$\varphi_m \in \{-60, -40, -20, 0, 20, 40, 60\}$
	Distance (km)	dis $\in \{5, 6, 7, 8, 9, 10, 11, 12, 13, 14, 15\}$

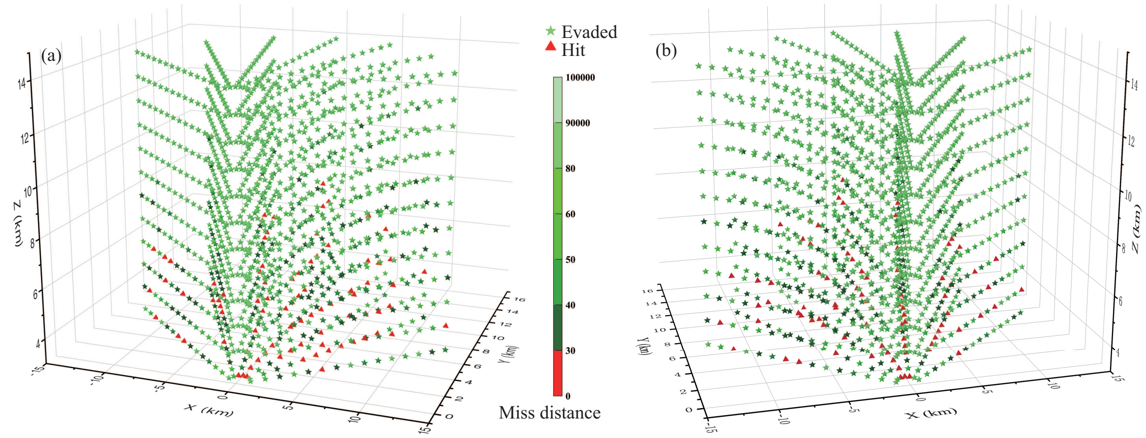

Figure 10 (Color online) Maneuvering results in different initial missile states. (a) View from the left; (b) view from the right.

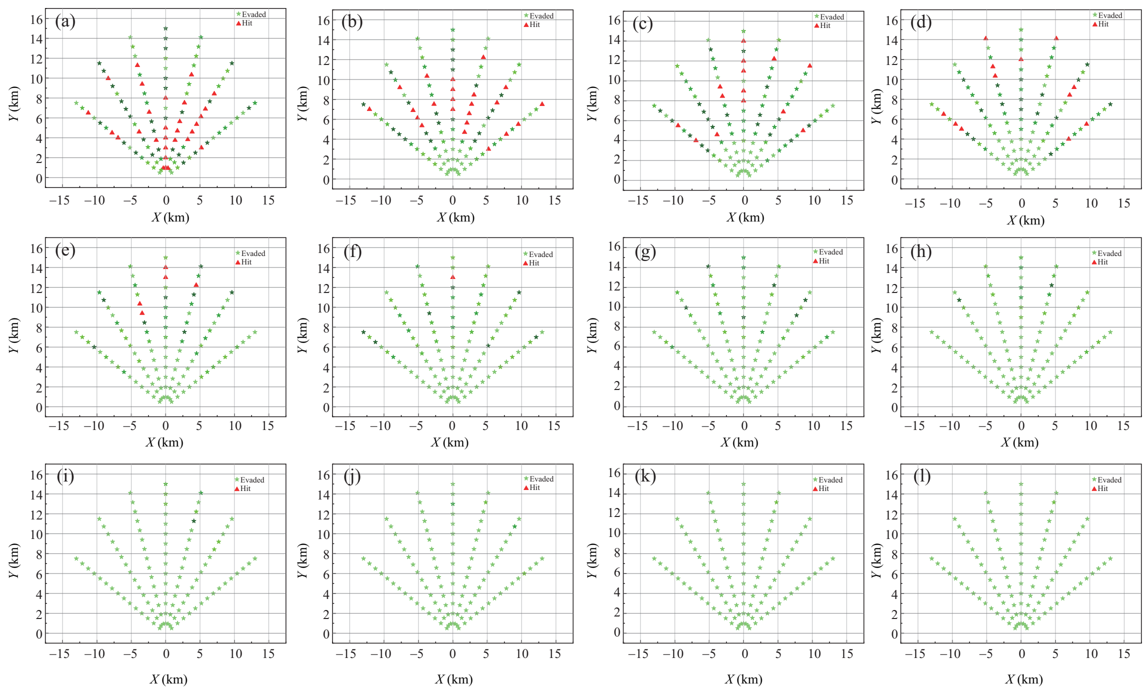

Figure 11 (Color online) Optimal evasion results at different initial altitudes of the missile. (a) $z_m = 3$ km; (b) $z_m = 4$ km; (c) $z_m = 5$ km; (d) $z_m = 6$ km; (e) $z_m = 7$ km; (f) $z_m = 8$ km; (g) $z_m = 9$ km; (h) $z_m = 10$ km; (i) $z_m = 11$ km; (j) $z_m = 12$ km; (k) $z_m = 13$ km; (l) $z_m = 14$ km.

for the missile to quickly lock on the plane, allowing the plane to have more time to react. Furthermore, the plots are approximately symmetrical when considering both the left and the right sides, demonstrating that the difficulty in avoiding an incoming missile is the same from both directions.

5 Conclusion

This study proposes an optimal evasive maneuver using the FQM. The simplified dynamics model of the plane is constructed to substitute for the traditional 6-DOF model. Furthermore, a missile model employing the proportional guidance law is formulated to attack the plane. Subsequently, an optimization problem is established to determine the optimal evasion trajectory, which is verified through simulation. The results thus obtained prove the effectiveness of the proposed simplified model and optimization algorithm. For future work, the evolutional methods such as deep reinforcement learning will be used to solve the optimization problem, while the intelligent controller design [37, 38] can be further considered during the command tracking.

Acknowledgements The work was supported by National Natural Science Foundation of China (Grant No. 61933010) and Natural Science Basic Research Plan in Shaanxi Province (Grant No. 2023JC-XJ-08).

References

1 Bai T T, Wang D B. Cooperative trajectory optimization for unmanned aerial vehicles in a combat environment. Sci China Inf Sci, 2019, 62: 010205

2 Ding J F, Si G Y, Ma J, et al. Mission evaluation: expert evaluation system for large-scale combat tasks of the weapon system of systems. Sci China Inf Sci, 2018, 61: 012106

3 Borck H, Karneeb J, Alford R, et al. Case-based behavior recognition in beyond visual range air combat. In: Proceedings of the 28th International Flairs Conference, 2015

4 Ramirez M, Papasimeon M, Lipovetzky N, et al. Integrated hybrid planning and programmed control for real time UAV maneuvering. In: Proceedings of the 17th International Conference on Autonomous Agents and Multiagent Systems, 2018. 1318–1326

5 Li S, Chen M, Wang Y, et al. Air combat decision-making of multiple UCAVs based on constraint strategy games. Defence Tech, 2022, 18: 368–383

6 Ruan W, Duan H, Deng Y. Autonomous maneuver decisions via transfer learning pigeon-inspired optimization for UCAVs in dogfight engagements. IEEE CAA J Autom Sin, 2022, 9: 1639–1657

7 McGrew J S, How J P, Williams B, et al. Air-combat strategy using approximate dynamic programming. J Guidance Control Dyn, 2010, 33: 1641–1654

8 Piao H, Han Y, Chen H, et al. Complex relationship graph abstraction for autonomous air combat collaboration: a learning and expert knowledge hybrid approach. Expert Syst Appl, 2023, 215: 119285

9 Wang L, Guo Y, Zhang Q, et al. Suggestion for aircraft flying qualities requirements of a short-range air combat mission. Chin J Aeronautics, 2017, 30: 881–897

10 Xie R, Li J, Luo D. Research on maneuvering decisions for multi-UAVs air combat. In: Proceedings of the 11th IEEE International Conference on Control & Automation (ICCA), 2014. 767–772

11 Wang Q, Wang Y Z. Cluster synchronization of a class of multi-agent systems with a bipartite graph topology. Sci China Inf Sci, 2014, 57: 012203

12 Sun Z, Piao H, Yang Z, et al. Multi-agent hierarchical policy gradient for air combat tactics emergence via self-play. Eng Appl Artif Intelligence, 2021, 98: 104112

13 Ma L, Lin B, Zhang W, et al. A survey of research on the distributed cooperation method of the UAV swarm based on swarm intelligence. In: Proceedings of IEEE 13th International Conference on Software Engineering and Service Science (ICSESS), 2022. 305–309

14 Hu J, Wang L, Hu T, et al. Autonomous maneuver decision making of dual-UAV cooperative air combat based on deep reinforcement learning. Electronics, 2022, 11: 467

15 Kong W, Zhou D, Yang Z, et al. Maneuver strategy generation of UCAV for within visual range air combat based on multi-agent reinforcement learning and target position prediction. Appl Sci, 2020, 10: 5198

16 Huang C Q, Dong K S, Huang H Q, et al. Autonomous air combat maneuver decision using Bayesian inference and moving horizon optimization. J Syst Eng Electron, 2018, 29: 86–97

17 Zhang R, Zhang J, Yu H. Review of modeling and control in UAV autonomous maneuvering flight. In: Proceedings of IEEE International Conference on Mechatronics and Automation (ICMA), 2018. 1920–1925

18 Austin F, Carbone G, Falco M, et al. Automated maneuvering decisions for air-to-air combat. In: Proceedings of Guidance, Navigation and Control Conference, 1987. 2393

19 Park H, Lee B Y, Tahk M J, et al. Differential game based air combat maneuver generation using scoring function matrix. Int J Aeronaut Space Sci, 2016, 17: 204–213

20 Liu P, Ma Y. A deep reinforcement learning based intelligent decision method for UCAV air combat. In: Proceedings of Asian Simulation Conference, 2017. 274–286

21 Horie K, Conway B A. Optimal fighter pursuit-evasion maneuvers found via two-sided optimization. J Guidance Control Dyn, 2006, 29: 105–112

22 Karelahti J, Virtanen K, Raivio T. Near-optimal missile avoidance trajectories via receding horizon control. J Guidance Control Dyn, 2007, 30: 1287–1298
23 Wang Z, Li H, Wu H, et al. Improving maneuver strategy in air combat by alternate freeze games with a deep reinforcement learning algorithm. Math Problems Eng, 2020, 2020: 1–17
24 Ong S Y, Pierson B L. Optimal evasive aircraft maneuvers against a surface-to-air missile. In: Proceedings of the 1st IEEE Regional Conference on Aerospace Control Systems, 1993. 475–482
25 Turetsky V, Shinar J. Missile guidance laws based on pursuit-evasion game formulations. Automatica, 2003, 39: 607–618
26 Imado F, Kuroda T. Family of local solutions in a missile-aircraft differential game. J Guidance Control Dyn, 2011, 34: 583–591
27 Carr R W, Cobb R G, Pachter M, et al. Solution of a pursuit-evasion game using a near-optimal strategy. J Guidance Control Dyn, 2018, 41: 841–850
28 Imado F, Kuroda T. Engagement tactics for two missiles against an optimally maneuvering aircraft. J Guidance Control Dyn, 2011, 34: 574–582
29 Hu J, Prandini M, Sastry S. Optimal coordinated maneuvers for three-dimensional aircraft conflict resolution. J Guidance Control Dyn, 2002, 25: 888–900
30 Yang Q, Zhu Y, Zhang J, et al. UAV air combat autonomous maneuver decision based on DDPG algorithm. In: Proceedings of IEEE 15th International Conference on Control and Automation (ICCA), 2019. 37–42
31 Liu G, Li B, Ji Y. A modified HP-adaptive pseudospectral method for multi-UAV formation reconfiguration. ISA Trans, 2022, 129: 217–229
32 Xin B, Chen J, Peng Z H, et al. An adaptive hybrid optimizer based on particle swarm and differential evolution for global optimization. Sci China Inf Sci, 2010, 53: 980–989
33 Imado F. Some practical approaches to pursuit-evasion dynamic games. Cybernetics Syst Anal, 2002, 38: 276–291
34 Chong E K, Zak S H. An Introduction to Optimization. Hoboken: John Wiley & Sons, 2013
35 Singh A. An overview of the optimization modelling applications. J Hydrol, 2012, 466–467: 167–182
36 Huntington G T, Rao A V. Optimal reconfiguration of spacecraft formations using the Gauss pseudospectral method. J Guidance Control Dyn, 2008, 31: 689–698
37 Xu B, Wang X, Sun F C, et al. Intelligent control of flexible hypersonic flight dynamics with input dead zone using singular perturbation decomposition. IEEE Trans Neural Networks Learn Syst, 2023, 34: 5926–5936
38 Xu B, Shou Y X, Wang X, et al. Finite-time composite learning control of strict-feedback nonlinear system using historical stack, IEEE Trans Cybern, 2023, 53: 5777–5787